ELSEVIER

Journal of Alloys and Compounds 230 (1995) 115–119

Journal of ALLOYS AND COMPOUNDS

The effect of cobalt and nickel on transformation in TiRh

Elena L. Semenova[a], V.M. Petyukh[a], Yu.V. Kudryavtsev[b]

[a]*I.N Frantsevich Institute for Problems of Material Science, Academy of Science of Ukraine, Krzhyzhanovsky str. 3, Kiev 252180, Ukraine*
[b]*Institute of Metal Physics, Academy of Science of Ukraine, Vernadsky str., Kiev 252142, Ukraine*

Received 6 February 1995; in final form 4 April 1995

Abstract

The transformations in TiRh and the effect of replacement of rhodium in TiRh by cobalt and nickel have been studied. TiRh undergoes two structural transformations which are of first order, exhibit thermoelastic properties and persist in the Ti–Rh–Co and Ti–Rh–Ni ternary alloys. Stabilization of the high temperature phase of TiRh of B2 type crystal structure down to room temperature can be achieved by substitution of cobalt at about 15 at.% and of nickel at about 20 at%. The TiCo–TiRh and TiNi–TiRh sections of the corresponding ternary systems are found to be quasi-binary.

Keywords: Co substitution; Ternary alloys; Transformations

1. Introduction

Taking into account the similarity of X-ray patterns of equiatomic phases at room temperature formed by transition metals of groups IV and VIII it was supposed that they undergo transformations like those observed in TiNi [1,2]. The latter is known to be accompanied by thermoelastic phenomena. The study of the TiPd, TiPt, ZrRh and ZrIr phases confirmed the correctness of this supposition, with the transformation temperature being higher than that for TiNi [3–5]. The TiRh compound was found to reveal two transformations [6,7]. The first, B2–$L1_0$ occurs at about 740 °C, and the second, $L1_0$–monoclinic, at about 345 °C on cooling [7]. This paper is the continuation of the experimental studies of these transformations in TiRh and of the influence of the substitution of rhodium for cobalt and nickel on both the transformation character and the temperatures. The rhodium atoms seemed likely to substitute for cobalt and nickel atoms in the B2 lattice sites because of similarities in sizes and electronic structure.

2. Experimental Procedure

The starting metals used for alloying were iodized titanium, nickel (99.95), cobalt (99.95) and rhodium powder (99.97). The rhodium powder was annealed in vacuum and remelted in order to avoid further sputtering during alloying. The alloys were prepared directly by arc-melting from components under an atmosphere of purified argon gas in a furnace with a non-consumable electrode on a water-cooled copper bottom. The weight losses on melting were small (below 0.3%) so nominal compositions are reported. The alloys, as cast and heat treated, were subjected to the differential thermal analysis (DTA) and X-ray and metallographic examinations [8,9]. The transformation temperatures in the TiRh-based alloys were determined by DTA and electrical resistance measurements. The shape memory effect (SME) was examined by the bending technique by thermocycling through the transformation range [10].

3. Results and discussion

3.1. TiRh

Metallographic examination reveals a lenticular structure in the equiatomic TiRh as-cast alloy at room temperature (Fig. 1). It is known that such a morphology is associated with compounds of the B2-type crystal structure at high temperatures, which reveal a martensitic transformation on cooling [11]. The dependence of the electric resistance of TiRh on temperature shows that there are two transformations in it

SSDI 0925-8388(95)01661-9

Fig. 1. Microstructure of as-cast TiRh. (Magnification, 100×.)

(Fig. 2, curve 1). The first, at higher temperature, occurs without hysteresis (the hysteresis, which is less than 1 °C, is not observed in our experiment); the second, at low temperature, occurs with a small hysteresis. Therefore the beginning and the end of the transformation on heating and cooling almost coincide ($M_s^I \approx A_f^I \approx 740$ °C; $M_f^I \approx A_s^I \approx 600$ °C; $M_s^{II} \approx A_f^{II} \approx 345$ °C; $M_f^{II} \approx A_s^{II} + 140$ °C) (Table 1). Two thermal effects were obtained by DTA for TiRh corresponding to those transformations. It proves not only the correctness of the temperatures mentioned but also testifies that both transformations are of the first order.

SME in TiRh was observed for the low temperature transformation (Fig. 3) (the mechanical test in the high temperature range was not carried out because of experimental complications). An almost complete shape restoration determined by bending tests was found. The critical points of transformation differ somewhat from those obtained by the electrical resistance method because of the large extent of the hysteresis. At temperatures exceeding 350 °C, owing to a decrease in elastic constants of the phase formed with increasing temperature, the bending of the sample should persist or increase slightly whereas in the experiment a further straightening of the sample was observed. This means that the process of shape restoration is retained after reverse transformation. Such behavior of accumulation and return of the deformation in TiRh shows that SME applies to the high temperature transformation as well. The X-ray analysis of the equiatomic TiRh alloy at room temperature revealed an imperfect crystal structure with the lattice parameters $a = 4.17$ Å, $c = 3.335$ Å close to known tetragonal CuAu-type structure. It was assumed in Ref. [7] that its structure is tetragonal with a monoclinic distortion. In Ref. [12] the occurrence of two transformations in TiRh was confirmed by high temperature X-ray diffraction and the following crystal

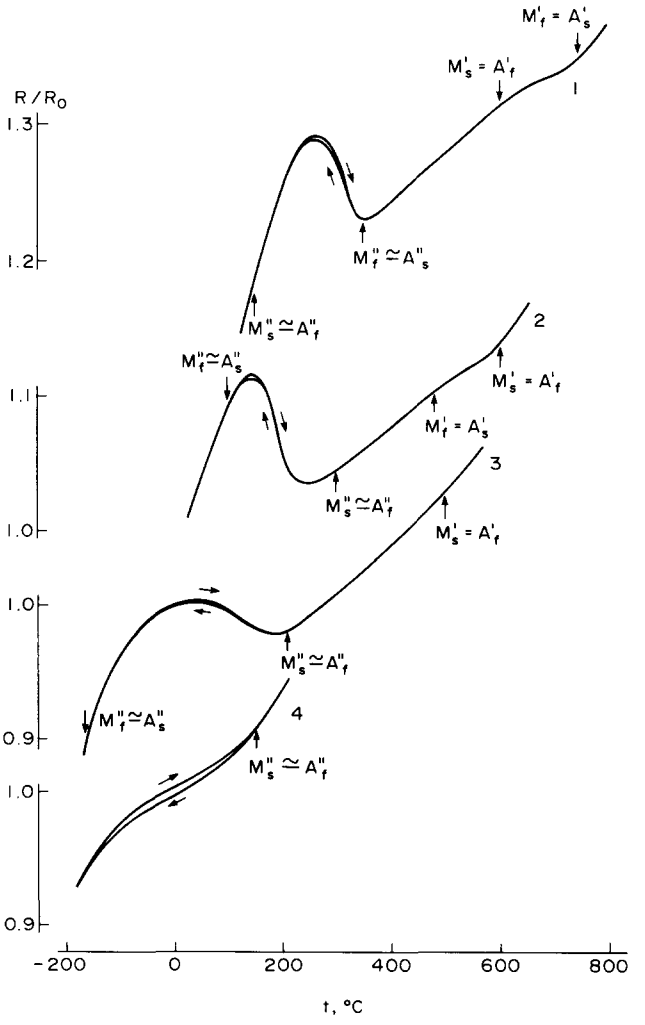

Fig. 2. Variation in electrical resistance on temperature for alloys: curve 1, TiRh; curve 2, with 5 at.% Co; curve 3, with 10 at.% Co; curve 4, with 15 at.% Co; M_s^I, M_f^I, A_s^I, A_f^I, the first stage transformation temperatures; M_s^{II}, M_f^{II}, A_s^{II}, A_f^{II}, the second stage transformation temperatures.

Table 1
The transformation temperatures of the Ti–Rh–Co and Ti–Rh–Ni system alloys

Composition of alloy (at.%)	$M_s^I = A_f^I$ (°C)	$M_f^I = A_s^I$ (°C)	M_s^{II} (°C)	M_f^{II} (°C)	A_s^{II} (°C)	A_f^{II} (°C)
TiRh	740	600	345	140	140	345
4Co	650	—	300	150	150	300
10Co	430	—	150	100	130	175
14Co	315	—	94	50	110	150
20Co	200	—	—	—	—	—
5Ni	600	480	300	300	100	100
10Ni	500	—	210	—	—	—
15Ni	—	—	150	—	—	150

structures of the transformation products were found: cubic, B2 type ($a = 3.126$ Å, 1000 °C) → tetragonal $L1_0$ type (CuAu) ($a = 4.226$ Å, $c = 3.350$ Å, 83 °C) → monoclinic ($a = 4.178$ Å, $b = 4.185$ Å, $c = 3.371$ Å; $\beta =$

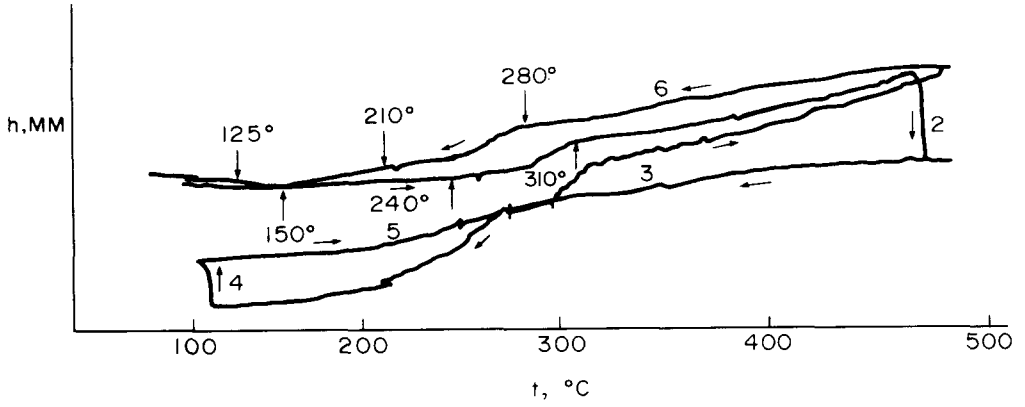

Fig. 3. Dependence of the TiRh sample bending on temperature: curve 1, free heating; curve 2, loading; curve 3, cooling under load; curve 4, removal of load; 5, heating without load.

90.89 °C). Taking into consideration the strong dependence of the degree of the lattice distortion (cubic → tetragonal → orthorhombic → monoclinic) [6,13] on the composition of the TiRh phase through its homogeneity range (about 5%), the difference in X-ray data obtained by us and in Refs. [6,12] can be explained. Thus it can be accepted that the TiRh compound on cooling from subsolidus temperatures to room temperature undergoes two consistent phase transformations of the martensitic type according to the scheme δ_1 (B2) → δ_2 ($L1_0$) → δ_3 (monoclinic).

3.2. TiRh–TiCo

It is known that the TiCo compound has the B2-type crystal structure which is stable from the subsolidus point to room temperature. The ternary alloys with 5, 10, 15, 30, 40 at.% Co have been studied in the TiCo–TiRh system. The high thermodynamic stability of the TiCo and TiRh compounds ($\Delta H^{for}_{TiCo} = -44$ kJ mol [14]; $\Delta H^{for}_{TiRh} = -143$ kJ mol^{-1} [15]) was expected to lead to a quasi-binary in the TiRh–TiCo section of the Ti–Rh–Co system. The TiRh–TiCo melting data obtained confirm this. There are continuous solidus and liquidus curves (Fig. 4(a)). The corresponding temperatures increase gradually from 1580 °C (TiCo) to 1960°C (TiRh). Such a type of melting diagram is attributed to the formation of solid solutions between the phases on the basis of TiCo and TiRh with B2-type crystal structure (δ_1). The replacement of rhodium by 15 at.% Co results in a stabilization of the δ_1 phase at room temperature together with a martensitic phase. Complete stabilization of the δ_1 phase is observed in the alloy with 20 at.% Co. The lattice period of the δ_1 phase increases at rhodium substitution from 2.988 Å for TiCo to 3.060 Å for the alloy with 20 at.% Rh.

The dependence of the resistance on temperature of Ti–Rh–Co alloys is shown in fig. 2. According to these data two transformations in the solid state are found. These are similar to those of the TiRh compound for the alloy with 45 at.% Rh. The first transformation is without hysteresis (below 1 °C); the second has a small hysteresis of about 10 °C (Table 1). These two transformations have also been observed by DTA. Both are transformations of first order.

When the cobalt content increases, the temperature of the onset of the first martensitic transformation decreases. Simultaneously its temperature interval starts to broaden, assuming that the premartensitic character changes before the second transformation. Its intensity decreases with increasing cobalt content.

3.3. TiRh–TiNi

We have studied 11 alloys in this system. The thermodynamic data for both TiNi, $\Delta H^{for}_{TiNi} = -34$ kJ mol^{-1} [16], and TiRh, mentioned above, indicate a relatively high stability of these compounds in the corresponding binary systems, so that the TiNi–TiRh section of the Ti–Rh–Ni ternary system should be quasi-binary as well as it is in case of the Ti–Rh–Co system. The TiRh–TiNi melting curves go up uninterruptedly from 1310 (TiNi) to 1960 °C (TiRh), which shows that continuous solid solutions are formed during the crystallization of the TiRh–TiNi alloys (Fig. 4(b)). The high temperature phase of TiNi is known to have a cubic B2-type crystal structure as TiRh has at subsolidus temperatures. Therefore TiRh–TiNi alloys should also be cubic (δ_1) at those temperatures. The δ_1 phase is stabilized down to room temperature in alloys with 6–30 at.% Rh. Its lattice period increases from 3.030 Å to 3.066 Å in this concentration range. Extrapolating these values to the equiatomic alloy (50 at.% Rh) leads to a TiRh lattice parameter of

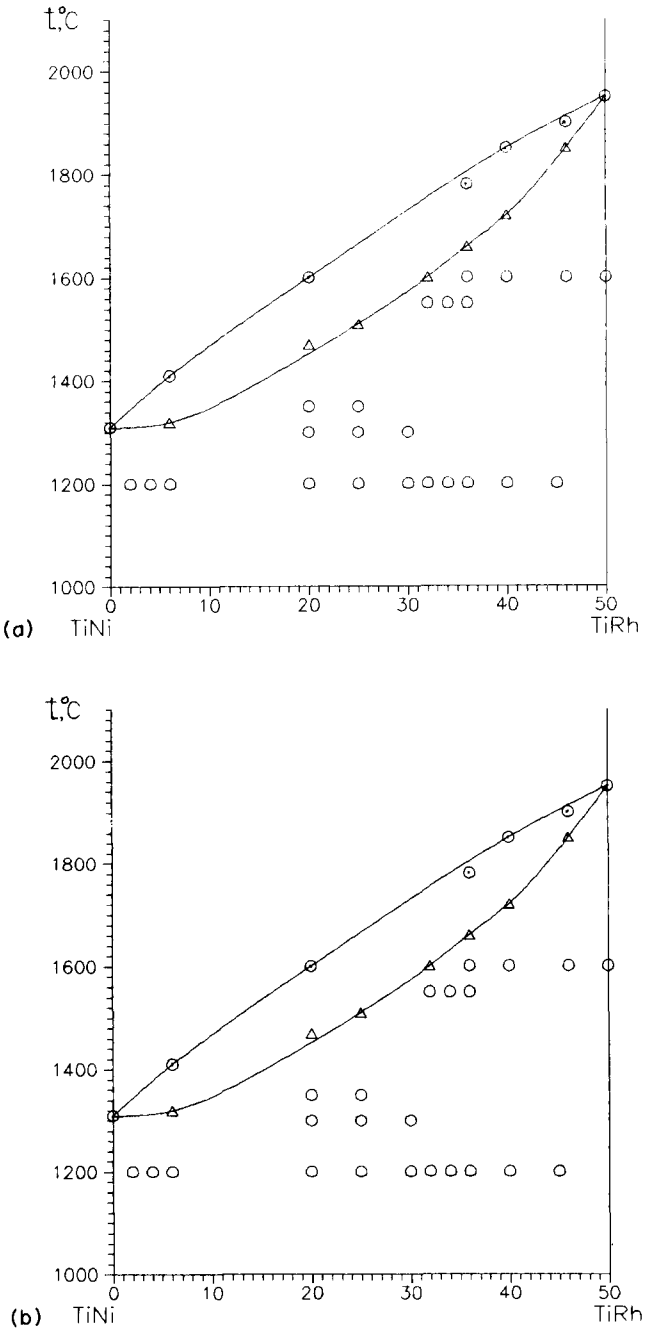

Fig. 4. (a) TiCo–TiRh phase diagram; (b) TiNi–TiRh phase diagram; ⊙, liquidus temperature; △, solidus temperature; ○, single-phase alloys.

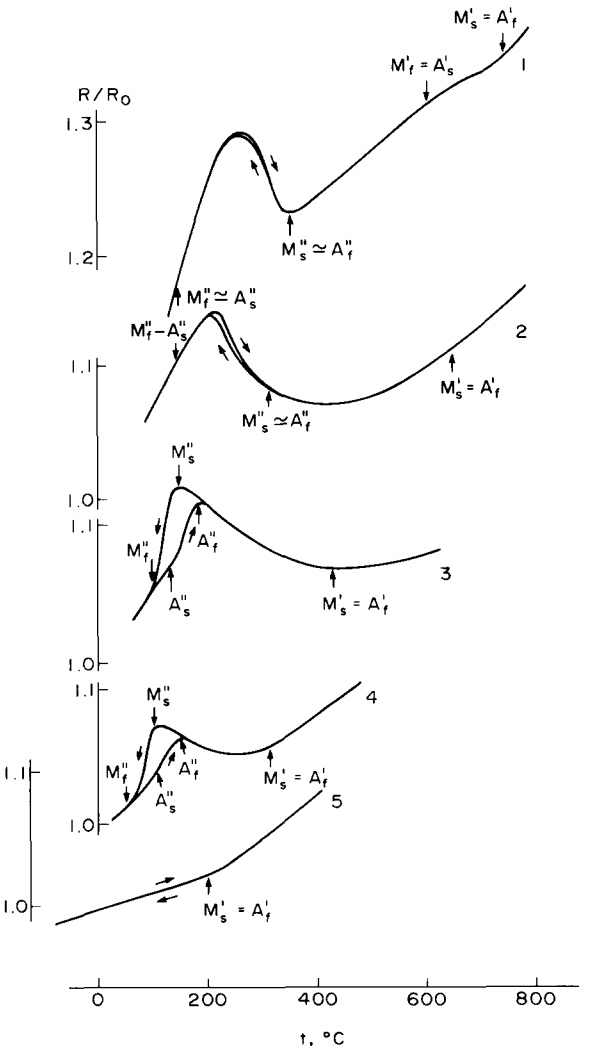

Fig. 5. Variation in the electrical resistance on temperature for the alloys: curve 1, TiRh; curve 2, with 4 at.% Ni; curve 3, with 10 at.% Ni; curve 4, with 14 at% Ni; curve 5, with 18 at.% Ni; other symbols as for Fig. 2.

3.13 Å. This value is equal to that for Ti–Rh–Co alloys obtained in a similar way and the value in Ref. [12], obtained by the direct method.

As we can see from the electrical resistance data (Fig. 5, curve 2; Table 1) two transformations were found in the alloy with 4% Ni on cooling. They occur in the same sequence $\delta_1 \rightarrow \delta_2 \rightarrow \delta_3$ as for the TiRh alloy.

However, the low temperature transformation character for alloys with higher nickel content changes significantly. The temperature dependence of R/R_0 becomes reversed (Fig. 5, curve 4): the decrease in the electrical resistance corresponds to the transformation on cooling. The alloy with 10% Ni reveals the phase with f.c.c. crystal structure ($a = 3.80$ Å) at room temperature. It was found by a high temperature investigation that at 520 °C its crystal structure is cubic, B2 type ($a = 3.09$ Å). This temperature (520 °C) corresponds to that obtained by the electrical resistance method. The cause of the differences in transformation behaviour of alloys with 4% and 10% Ni can be an ordering that takes place when substituting rhodium for nickel. The scheme of the phase structure transformations in the TiRh–TiCo, TiRh–TiNi alloys on the side of TiRh which demonstrates the influence of the substitution of Rh for Co, Ni on both tempera-

ture and concentration in the δ_1 and δ_2 phase regions is shown in Fig. 6. The two-stage processes are displayed on curves of temperature vs. composition. The substitution for Co decreases the transformation temperature M_s^I more strongly than for Ni. The replacement of rhodium by both cobalt and nickel in TiRh results in a displacement of M_s^I and M_s^{II} at the lower temperature side but the decrease in the temperature M_s^I occurs more strongly in both cases. The scheme of the phase structure transformation for TiNi was constructed previously [17]. The rhodium additions to TiNi lead to a decrease in all martinsitic transformation temperatures, and all peculiarities of the martensitic transformation observed in the binary TiNi alloy are preserved.

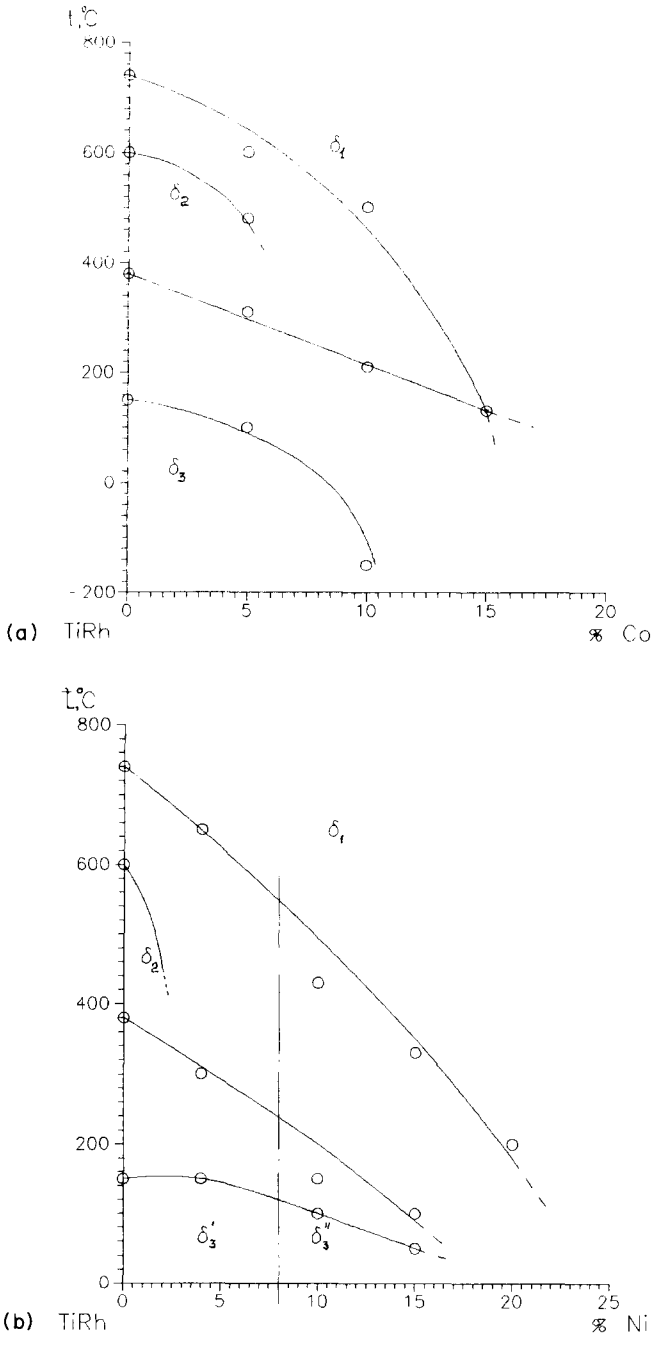

Fig. 6. Scheme of the structural transformation in the Ti–Rh–Co and Ti–Rh–Ni ternary alloys on the Rh-rich side of TiRh.

References

[1] F.E. Wang, *J. Appl. Phys., 38* (1967) 822.
[2] F.E. Wang, D.W. Ernst, *J. Appl. Phys., 39* (1968) 2192.
[3] V.N Khachin, N.M. Matveeva, V.P. Sivokha, et al., *Dokl. Akad. Nauk USSR, 257* (1981) 167.
[4] N.M. Matveeva, I.E. Luboserdova, V.N. Khachin, et al., in *Alloys of Rare Metals with Particular Physical Properties*, Nauka, Moscow, 1983, p. 163.
[5] E.L. Semenova and Yu.V. Kudryavtsev, *J. Alloys Compd., 203* (1994) 165.
[6] P. Rogl, in K.I. Komarek (ed.), *Atomic Energy Review*, Special Issue 9, International Atomic Energy Agency, Vienna, p. 201.
[7] Yu.V. Kudryavtsev, E.L. Semenova and L.A. Tretyachenko, in *The Stable and Metastable Phases in Materials*, IPM, Kiev, 1987, p. 138.
[8] V.N. Yeremenko, E.L. Semenova, T.D. Shtepa and Yu.V. Kudryavtsev, *Dokl. Akad. Nauk Ukr. RSR, Ser. A, 10* (1978) 943.
[9] V.N. Yeremenko, E.L. Semenova, V.G. Choruzaja and T.D. Shtepa, in *Physical Chemistry of Inorganic Materials*, Vol. 1, Naukova Dumka, Kiev, 1988, p. 275.
[10] I.A. Arbuzova, Yu.N. Koval, V.V. Martynov and L.G. Khandros, *Fiz. Met. Metalloved., 35* (1973) 1278.
[11] A.E. Dwight, *Trans. Metall. Soc. AIME, 215* (1959) 283.
[12] S.S. Yi, B.H. Chen and F.F. Franzen, *J. Less-Common Met., 143* (1988) 243.
[13] T.D. Shtepa, in *Physical Chemistry of Condense Phases, Superhard Materials and their Boundaries of Separate*, Naukova Dumka, Kiev, 1975, p. 175.
[14] A.K. Niessen, A.R. Miedema, F.R. de Boer and R. Boom, *Physica B, 151* (1988) 401.
[15] L. Topor, O.J. Kleppa, *J. Less-Common Met., 155* (1989) 61.
[16] A.K. Niessen, A.R. Miedema, F.R. de Boer and R. Boom, *Physica B, 152* (1988) 303.
[17] A.A. Klopotov, Yu.A. Sazanov, Yu.V. Kudryavtsev and E.L. Semenova, *Izv. Vyssh. Uchebn. Zaved., Ser. Fiz., 8* (1991) 44.